Journal of Affective Disorders 294 (2021) 847–856

Contents lists available at ScienceDirect

Journal of Affective Disorders

journal homepage: www.elsevier.com/locate/jad

Research paper

Brain controllability distinctiveness between depression and cognitive impairment

Feng Fang [a], Yunyuan Gao [b,**], Paul E. Schulz [c], Sudhakar Selvaraj [d], Yingchun Zhang [a,*]

[a] Department of Biomedical Engineering, University of Houston, Houston, TX, USA
[b] Department of Intelligent Control & Robotics Institute, College of Automation, Hangzhou Dianzi University, Hangzhou 310018, China
[c] Department of Neurology, The McGovern Medical School of UT Health Houston, Houston, TX, USA
[d] Department of Psychiatry and Behavioral Sciences, The McGovern Medical School of UT Health Houston, Houston, TX, USA

ARTICLE INFO

Keywords:
Diffusion tensor imaging
Structural network
Brain controllability
Cognitive impairment
Depression

ABSTRACT

Alzheimer's disease (AD) is a progressive form of dementia marked by cognitive and memory deficits, estimated to affect ~5.7 million Americans and account for ~$277 billion in medical costs in 2018. Depression is one of the most common neuropsychiatric disorders that accompanies AD, appearing in up to 50% of patients. AD and Depression commonly occur together with overlapped symptoms (depressed mood, anxiety, apathy, and cognitive deficits.) and pose diagnostic challenges early in the clinical presentation. Understanding their relationship is critical for advancing treatment strategies, but the interaction remains poorly studied and thus often leads to a rapid decline in functioning. Modern systems and control theory offer a wealth of novel methods and concepts to assess the important property of a complex control system, such as the brain. In particular, the brain controllability analysis captures the ability to guide the brain behavior from an initial state (healthy or diseased) to a desired state in finite time, with suitable choice of inputs such as external or internal stimuli. The controllability property of the brain's dynamic processes will advance our understanding of the emergence and progression of brain diseases and thus helpful in the early diagnosis and novel treatment approaches. This study aims to assess the brain controllability differences between mild cognitive impairment (MCI), as prodromal AD, and Depression. This study used diffusion tensor imaging (DTI) data from 60 subjects from the Alzheimer's Disease Neuroimaging Initiative (ADNI): 15 cognitively normal subjects and 45 patients with MCI, including 15 early MCI (EMCI) patients without depression, 15 EMCI patients with mild depression (EMCID), and 15 late MCI (LMCI) patients without depression. The structural brain network was firstly constructed and the brain controllability was characterized for each participant. The controllability of default mode network (DMN) and its sub-regions were then compared across groups in a structural basis. Results indicated that the brain average controllability of DMN in EMCI, LMCI, and EMCID were significantly decreased compared to healthy subjects ($P < 0.05$). The EMCI and LMCI groups also showed significantly greater average controllability of DMN versus the EMCID group. Furthermore, compared to healthy subjects, the regional controllability of the left/right superior prefrontal cortex and the left/right cingulate gyrus in the EMCID group showed a significant decrease ($P < 0.01$). Among these regions, the left superior prefrontal region's controllability was significantly decreased ($P < 0.05$) in the EMCID group compared with EMCI and LMCI groups. Our results provide a new perspective in understanding depressive symptoms in MCI patients and provide potential biomarkers for diagnosing depression from MCI and AD.

1. Introduction

Alzheimer's disease (AD) is the most common cause of dementia, characterized by cognitive and memory deficits and accounted for ~$277 billion in medical costs in 2018 (A. s. Association, 2018). Its onset is marked by neurocognitive control disturbances, including memory loss, disinterest, trouble concentrating, and low motivation (Minati et al., 2009; Li et al., 2018; Luo et al., 2020). AD patients often develop

* Corresponding authors: Department of Biomedical Engineering, University of Houston, 4849 Calhoun Rd. Rm 373, Houston, TX 77004 USA.
** Co-corresponding authors.
E-mail address: yzhang94@uh.edu (Y. Zhang).

https://doi.org/10.1016/j.jad.2021.07.106
Received 19 May 2021; Received in revised form 22 July 2021; Accepted 26 July 2021
Available online 31 July 2021

significant neuropsychiatric symptoms that exacerbate deficits (Luo et al., 2021). Depression is currently acknowledged as the primary neuropsychiatric symptom of AD, appearing in up to 50% of AD patients (Chi et al., 2014). Unfortunately, depression also appears as a common, independent mood disorder in the elderly population, with symptoms that often overlap with AD (such as depressed mood, anxiety, apathy, cognitive deficits.) (A. P. Association, 2013). This overlap makes it difficult to determine whether symptomatic individuals have developed depression, are in the early stages of cognitive decline, or are suffering from the combined effects of both (Dillon et al., 2014). Moreover, the allostatic load that depression presents may worsen cognitive decline and increase the risk for AD development (Ownby et al., 2006). At present, a "wait and see" approach is often taken; however, the underlying neural alterations of AD begin before the cognitive decline and a passive monitoring approach would significantly delay treatment (Beason-Held et al., 2013). It is therefore of great clinical importance to identify the unique properties of individuals with mild cognitive impairment (MCI), as prodromal AD, with and without comorbid depression, to improve diagnostic methods and guide effective treatment.

Several neuroimaging modalities, including Fluorodeoxyglucose Positron Emission Tomography (FDG-PET), functional magnetic resonance imaging (fMRI), and diffusion tensor imaging (DTI), have been employed to study MCI and depression and have found functional alterations in several brain regions (Yu et al., 2019; Lee et al., 2010; Liu et al., 2017; Byers and Yaffe, 2011). MCI patients with depression show lower glucose metabolism in the superior frontal gyrus than MCI patients without depression (Lee et al., 2010). Resting-state fMRI measurements were used to explore the temporal variability of intrinsic brain activity to identify the brain functional activity differences in two groups of MCI patients (with and without depression) (Yu et al., 2019). The results indicated that MCI patients with depression had a decreased capability of integrating distributed neural populations and brain areas, thereby changing the synchronization patterns of the brain after receiving an internal or external stimulus (Yu et al., 2019). A recent DTI study revealed that the structural impairments in the cortico-subcortical networks are related to affect regulation and reward /aversion control of dementia patients with depression (Byers and Yaffe, 2011). Moreover, the graph-based measures, such as node strength, betweenness centrality, and global efficiency, were also used to explore the MCI patients with depression from a network perspective (Liu et al., 2017). Graph measures have been employed in various studies to explore the brain dynamic network behaviors (Fang et al., 2020,; Nguyen et al., 2019,; Sporns, 2018). For instance, the MCI patients with depression were reported to have reduced whole-brain global efficiency and reduced local efficiency (Tumati et al., 2020).

The default mode network (DMN) is a pluripotent 'ground state', and therefore theoretically can control the proceeding of the brain behavior into many task-based activation profiles (Lin et al., 2017). The brain's default mode is also the state to which the brain relaxes after the task has been performed, readying the brain to move to new task states where the cycle can repeat (Gu et al., 2015). Its hubs include parts of the medial temporal lobe, prefrontal cortex, cingulate cortex, precuneus cortex, and parietal cortex (Öngür et al., 2010). Even though the DMN was usually interpreted in a functional basis, previous study also demonstrated that resting-state functional connectivity could reflect structural connectivity in the DMN (Greicius et al., 2009,; Guo et al., 2016). Two previous studies have used whole-brain DTI to discriminate participants with major depressive disorder (MDD) from participants without MDD based on DMN-related networks (Fang et al., 2012,; Korgaonkar et al., 2012). Recent studies have reported that the DMN is abnormal in dementia, the memory impairments observed in MCI, and depression (Burke et al., 2019). The topologically convergent and divergent structural connectivity patterns between depressive patients and MCI patients were also reported. For example, similar deficits of the regional and connectivity characteristics in the structural networks were primarily found in the frontal brain regions of depression and MCI patients compared with controls (Bai et al., 2012). Depression-related atrophy in DMN-related hubs such as the medial temporal gyrus (MTG), the superior prefrontal cortex (SPF), and the posterior cingulate cortex (CG), may also explain the disabling, and therefore intrinsically "dementing" nature of depressive illness (Wise et al., 2017,; Royall et al., 2013). However, the underlying control mechanisms of DMN and its related brain regions in dementia, especially associated with depression, have yet to be fully explored.

Network control theory has recently been applied to interpret brain state transitions, suggesting that brain controllability can be used to evaluate the ease of brain network transition from one state to another (Gu et al., 2015). Conventional graph-based measurements show the local properties of varied brain regions and their important roles in their network architecture (Sporns, 2018). Differently, control theory-based network measurements describe one brain region's ability to change the brain behavior from one state to another state, for example, from the brain executive state to the resting state, or maintain in a specific state, which is a systematic-level property (Tang et al., 2017,; Menara et al., 2018). Therefore, exploring the control properties of different brain regions and their correlation with the traditional graph measures may help us understand these regional hubs' functional roles and their critical roles in guiding the brain to move from any initial state to a desired state.

Patients with depression may experience a reduced capability to initiate, maintain, and control their thoughts, behaviors, or emotions, to change their brain states and produce the desired result or avoid an undesired outcome (Strauman and Eddington, 2017,; Taquet et al., 2020). Consequently, patients with depression are less susceptible to external mood-related salient stimuli, resulting in difficulty transiting to a state that motivates them to access the emotion or behavior. As brain states transition a critical part of cognitive control, network controllability can be used to explore the underlying control mechanism and neural circuits alterations of MCI patients with depression (Li et al., 2018). Overall, these novel network metrics of controllability allow us to assess the relative importance of different brain regions in modulating brain behaviors from the systematic level, thus offering a new perspective to better understand the pathologic differences in depression and MCI.

The goal of this study was to investigate the differences in the brain controllability between the early MCI patients without concurrent depression (EMCI) and with concurrent depression (EMCID), with particular attention being paid to the controllability of the DMN, which plays an important role in brain states transition. We hypothesize that the EMCID patients will have lower brain controllability in DMN and some cognitive-related regions than the other groups due to the superposition effect. To the best of our knowledge, this study represents the first effort to investigate depression symptom in MCI patients at a systematic level, which may lead to "systematic biomarkers" that can be employed for early diagnosis and intervention.

2. Materials and methods

2.1. Participants

All participants in this study were selected from the Alzheimer's Disease Neuroimaging Initiative (ADNI) dataset, available at http://adni.loni.usc.edu/. ADNI is a large, multi-site longitudinal study for evaluating biomarkers in Alzheimer's Disease (AD) and MCI patients. Written informed consent was obtained, as approved by the Institutional Review Board at each participating center.

The demographic data of the datasets are listed in Table 1. The schematic of brain controllability analysis steps is shown in Fig. 1. This study included 15 early MCI (EMCI) patients without depression, 15 late MCI (LMCI) patients without depression, 15 early MCI patients with depression (EMCID), and 15 cognitive normal subjects (CN). The

Table 1
Demographic data of CN, EMCI, EMCID, and LMCI subjects.

Variable	CN n = 15	EMCI n = 15	EMCID n = 15	LMCI n = 15	Group differences
Age	74.2 ± 8.2	78.5 ± 4.3	73.3 ± 7.6	72.6 ± 6.9	
Gender (M/F)	5/10	11/4	9/6	7/8	
MMSE	29.4 ± 0.9	27.7 ± 1.4	27.4 ± 2.3	26.8 ± 2.7	* † §
GDSCALE	1.8 ± 1.1	1.6 ± 0.9	5.5 ± 0.7	1.2 ± 1.5	† € ¶

Values represent mean ± SD. MMSE, Mini-Mental State Examination; GDSCALE, Geriatric Depression Scale.
* Group differences (P < .05, adjusted for multiple comparison): CN vs. EMCI
† Group differences (P < .05, adjusted for multiple comparison): CN vs. EMCID
§ Group differences (P < .05, adjusted for multiple comparison): CN vs. LMCI
€ Group differences (P < .05, adjusted for multiple comparison): EMCI vs. EMCID
¥ Group differences (P < .05, adjusted for multiple comparison): EMCI vs. LMCI
¶ Group differences (P < .05, adjusted for multiple comparison): EMCID vs. LMCI

criterion for the selection of MCI patients with and without depression was based on the Geriatric Depression Scale (GDSCALE) Total Score (Scale, 1997). Thus, from the ADNI dataset, the EMCI and LMCI patients were selected from the early MCI and late MCI groups, respectively, with GDSCALE Total Score between 0 and 4, and the EMCID patients were chosen from the early MCI group with GDSCALE Total Score between 5 and 8, which represent the EMCI patients with mild depression. All subjects underwent structural scanning on a 3 Tesla GE Medical systems machine according to the ADNI acquisition protocol. The LMCI group was included to evaluate the deficit level caused by depression in the EMCID group to ascertain whether depressive symptoms can cause worse brain dysfunction than the progressive effects of dementia. The EMCI and LMCI participants were classified by ADNI based on the WMS-R Logical Memory II Story A score (McGuire and Batchelor, 1998). The specific cutoff scores were as follows (out of a maximum score of 25): Early MCI (ADNI-EMCI) was assigned for a score of 9-11 for 16 or more years of education; a score of 5-9 for 8-15 years of education; or a score of 3-6 for 0-7 years of education. Late MCI (ADNI-LMCI) was assigned for a score of ≤ 8 for 16 or more years of eduction; a score of ≤ 4 for 8-15 years of education; or a score of ≤ 2 for 0-7 years of eduction (Edmonds et al., 2019).

2.2. Preprocessing

DTI data were preprocessed and reconstructed in DSI Studio (http://dsi-studio.labsolver.org/). Following prior methods (Gu et al., 2015), motion artifact and image distortions caused by eddy currents were firstly corrected. DTI data were then reconstructed using the q-space diffeomorphic reconstruction (QSDR) method (Yeh and Tseng, 2011). QSDR first reconstructed diffusion-weighted images in native space and computed the quantitative anisotropy (QA) in each voxel. These QA values were used to warp the brain to a template QA volume in Montreal Neurological Institute (MNI) space using the statistical parametric mapping (SPM) nonlinear registration algorithm. Once in MNI space, spin density functions were again reconstructed with a mean diffusion distance of 1.25 mm using three fiber orientations per voxel. Fiber tracking was performed in DSI studio with an angular cutoff of 90^0, step size of 1.0 mm, minimum length of 10 mm, spin density function smoothing of 0.0, and maximum length of 800 mm. Deterministic fiber tracking using a modified FACT algorithm was performed until 100,000 streamlines were reconstructed for each individual.

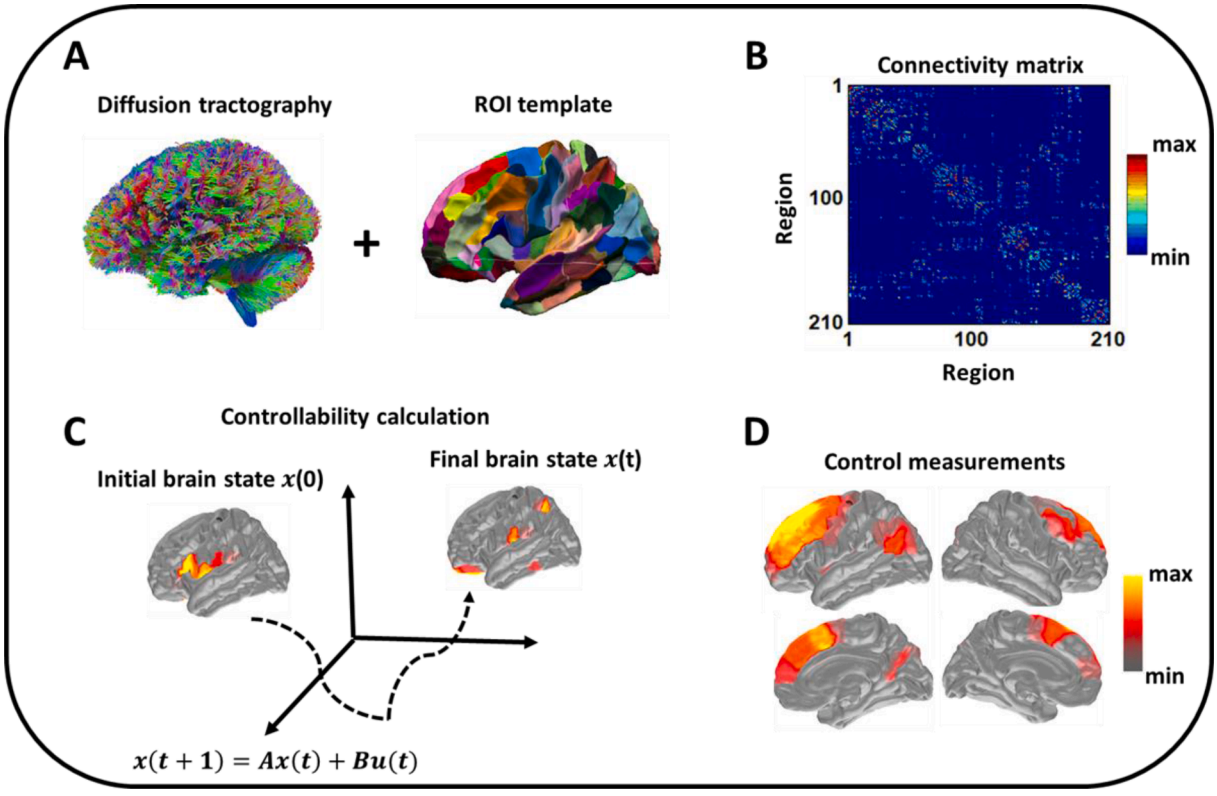

Fig. 1. Schematic of brain controllability analysis steps. (A) Diffusion tensor imaging measures the direction of water diffusion in the brain. From this data, white matter streamlines can be reconstructed that connect brain regions in a structural network. (B) Structural connectivity matrix indicating connections between different brain regions. Each element indicates the number of streamlines connecting two different brain regions. (C) From structural connectivity matrix, average controllability of each brain region can be calculated for each participant. (D) Visualize the brain controllability distribution map and quantify the controllability statistics.

Anatomical scans were segmented using FreeSurfer (https://surfer.nmr.mgh.harvard.edu/) and parcellated according to the Brainnetome atlas (https://atlas.brainnetome.org/). A parcellation scheme, including 210 cortical brain regions, was registered to the b0 volume from each subject's DTI data. Tractography was performed in DSI studio, and the number of streamlines connecting each pair of regions were used to weigh the edge connecting those regions and as the entries of the connectivity matrix.

2.3. Theory and calculation

In control theory, a dynamical system's controllability refers to the possibility of driving the state of a dynamical system to a specific target state using a control input (Gu et al., 2015). In contrast to traditional graph theory that provides descriptive statistics of network structure, network control theory offers mechanistic predictors of network dynamics. As for the brain, brain control can be thought of as the change in regional brain activity produced in response to real-time neurofeedback or the change in regional neural activity elicited by external stimuli or non-invasive brain stimulation (Gu et al., 2015). Each of these mechanisms initially alters the dynamics of single brain regions, but can have consequences for distributed networks' activity and function. Thus, the controllability measurement predicts each brain area's ability to transition the brain system from any initial state (healthy or disease), to any desired state in finite time. Following this, the task- and cognitive-control areas are thought to drive or constrain neurophysiological dynamics over distributed neural circuits using transient modulations, consistent with the role of engineering controllers (Tang et al., 2017).

One of the critical steps in applying network control theory to the human brain is to define a structural brain network and a model for the dynamics of neural processes. The streamline-weighted structural brain network was estimated from diffusion tractography based on DTI data. The weighted structural connectivity matrix A was defined as $A = [A_{ij}]$, where A_{ij} represents the number of streamlines connecting region i and region j. The elements in the diagonal of connectivity matrix A were set to zero, so no self-connection was considered. The method assumed that the number of streamlines between two brain regions is proportional to structural connectivity's strength regarding a proportion of activity between nodes (Gu et al., 2015). A simplified, noise-free linear time-invariant model of such dynamics can be formulated as follows:

$$x(t+1) = Ax(t) + B_K u_K(t) \quad (1)$$

where x with dimension N (number of regions) x 1 describes the state (that is, the magnitude of neurophysiological activity) of brain regions over time, and A with dimension N x N is the symmetric and weighted structural connectivity matrix as described above. The input matrix B_K with dimension N x m identifies the control points K in the brain, where $K = (k_1, \ldots, k_m)$ and $B_K = (e_{k_1}, \ldots, e_{k_m})$. e_i denotes the i-th canonical vector of dimension N, and m denotes the number of targeted nodes. The input u_k with dimension m x 1 denotes the external stimulation.

2.4. Controllability matrix and graph measures

Following the structural brain network and neural dynamic model's construction, the diagnostic of average controllability utilized in the previous network control studies was examined (Gu et al., 2015). The average controllability of a network equals the average input energy from a set of control nodes and overall possible target states (Sakha and Shaker, 2017). As a known result, average input energy is proportional to the trace of W_k^{-1}, the trace of the inverse of the controllability Gramian (Sreeram and Agathoklis, 1994). The controllability Gramian is defined as:

$$\mathrm{W_K} = \sum_{\tau=0}^{\infty} A^{\tau} B_k B_k^T A^{\tau} \quad (2)$$

To be consistent with prior studies, here we adopted the trace of $\mathrm{W_K}$ as a measure of average controllability. Therefore, the average controllability (a_c) can be mathematically described as:

$$a_c = Trace(\mathrm{W_K}) \quad (3)$$

The control nodes were chosen one at a time, and thus the input matrix B was reduced to a one-dimensional vector. Region with the highest average controllability is, on average, most influential in the control of network dynamics over all different target states (Gu et al., 2015).

To investigate the relationship between traditional static network metrics and controllability, we employed three graph measures that have already been explored to observe the intrinsic dysconnectivity pattern of AD and depression: node strength, betweenness, and global efficiency (Guo et al., 2016,; Berlot et al., 2016). In brief, the node strength is the sum of weights of links connected to the node. The node strength can help us understand whether the control hubs are located in strongly connected brain areas or sparsely connected areas. The betweenness centrality represents the fraction of all shortest paths in the network that pass through a given node, which identifies important nodes on a high proportion of paths between other nodes in the network. Betweenness may reveal the central roles of the control hubs in our brain network. The global efficiency indicates the integration of the network, representing the degree to which a network can share information between regions. This property is essential for us to understand whether a structural efficiency network is more controllable by an internal and external stimulus or not. All graph measure calculations were performed using the Brain Connectivity Toolbox (Rubinov and Sporns, 2010).

2.5. Statistical analysis

The average controllability distribution of different groups were statistically compared using one-way ANOVA and multiple comparisons were performed based on Wilcoxon signed-rank test (Woolson, 2007). A linear regression model was then used to explore each graph measure's relationship with the average controllability in each group, respectively (Poole and O'Farrell, 1971). The difference in overall average controllability in default mode network (DMN) between the E/LMCI, EMCID, and CN groups was statistically evaluated using one-way ANOVA. Wilcoxon signed-rank test was further employed to perform the post-hoc analysis. The statistical tests were corrected for multiple comparisons using the false discovery rate (FDR) correction (Benjamini and Hochberg, 1995). Regional controllability of a subset of regions in DMN (left/right medial temporal cortex, superior prefrontal cortex, and cingulate gyrus) were then compared between groups using Wilcoxon signed-rank test.

3. Results

3.1. Demographic and clinical behavioral data

Table 1 summarizes the demographic information and clinical behavioral scores of all cognitive normal subjects and patients, including age, gender, and clinical assessment scores. One-way ANOVA results revealed that there was no significant group difference in terms of age ($P > 0.05$), but significant group differences existed in terms of MMSE ($P < 0.05$) and GDSCALE ($P < 0.05$) scores. Chi-square test showed there was no significant group differences in terms of gender ($P > 0.05$). Multiple comparisons using one tail t-tests revealed significantly greater MMSE scores of the CN subjects versus the other groups ($P < 0.05$) and significantly greater GDSCALE scores in the EMCID group versus the others ($P < 0.05$). However, no significant differences in MMSE scores was observed between MCI groups ($P > 0.05$) and no significant differences was observed in GDSCALE scores between CN, EMCI, and LMCI groups ($P > 0.05$).

3.2. Controllability differences across the patient groups

The average controllability was computed for each subject and averaged over all subjects in each group, respectively. As shown in Fig. 2, the regions with high average controllability were mainly located in the left superior prefrontal cortex, left precentral cortex, left superior, middle temporal cortex, and right cingulate cortex. One-way ANOVA results revealed that there were significant group differences in the average controllability distributions between different MCI groups ($P < 0.05$). The Wilcoxon rank-sum test was employed to compare the controllability distribution of different MCI groups, as shown in Fig. 3. According to the p-value scale indicated in the color bar, the yellow color on the top of the brain represents a significant difference between the two MCI groups. The left occipital cortex showed a significant difference between the EMCI and LMCI groups ($P < 0.05$). One-tail Wilcoxon signed-rank test indicated that the average controllability of the left occipital cortex in the LMCI group was significantly greater than in the EMCI group ($P < 0.05$). Comparing the EMCI and EMCID groups, there were significant differences between the left/right superior prefrontal cortex, right inferior temporal cortex, and right postcentral cortex ($P < 0.05$). One-tail Wilcoxon signed-rank test indicated that the average controllability of these brain regions were significantly greater in the EMCI group versus the EMCID group ($P < 0.05$). The LMCI group showed a significant difference in regions of the left superior prefrontal cortex, left occipital cortex, and right postcentral cortex when compared with the EMCID group ($P < 0.05$), and one-tail Wilcoxon signed-rank test indicated that the average controllability of these brain regions were significantly greater in LMCI group than EMCID group ($P < 0.05$).

3.3. Correlation between the controllability and traditional graph-theory measures

The average controllability measurement was further compared with the traditional graph-theoretical measurements, as shown in Fig. 4. The correlation between controllability and node strength measure was high across the four groups (0.7687 ± 0.0650), with the highest r value of 0.85493 in the EMCID group. The node betweenness measurement showed a weak correlation with the controllability measure (0.3599 ± 0.0859). The global efficiency showed a strong correlation with controllability measurement (0.9029 ± 0.0557), with the lowest r-value of 0.8219 in the cognitively normal group.

Because of the high correlation between node strength and the controllability measurement, the distribution of node strength on the top of the brain was further visualized to check the similarity of the regional distribution between the two measurements (Fig. 5). The node strength distribution on the top of the brain showed a similar pattern as controllability measurement. The brain regions with high node strength are mainly located in the left superior prefrontal cortex, left precentral cortex, left/right inferior parietal area, right cingulate cortex, right medial temporal cortex, and right occipital area.

3.4. The controllability of default mode network (DMN) in different groups

The average controllability of the DMN was calculated from each subject and averaged over all subjects in each group. As shown in Fig. 6, the controllability of DMN in the cognitively normal group was significantly higher than all MCI groups. Moreover, the controllability of DMN in the EMCI and LMCI groups were both significantly higher than the EMCID group. No significant difference was observed between the EMCI and LMCI groups. The sub-regions of DMN were further compared, including left/right middle temporal cortex, left/right superior prefrontal cortex, and left/right cingulate cortex. The controllability of left/right superior prefrontal cortices and left/right cingulate cortices were significantly higher in the cognitively normal group than EMCID group. Among these regions, the controllability of the left superior prefrontal cortex in the EMCI and LMCI groups were both significantly higher than the EMCID group. The cognitive normal group also displayed significantly higher controllability in the right superior prefrontal cortex than LMCI group and significantly higher controllability in the right cingulate cortex than the EMCI group.

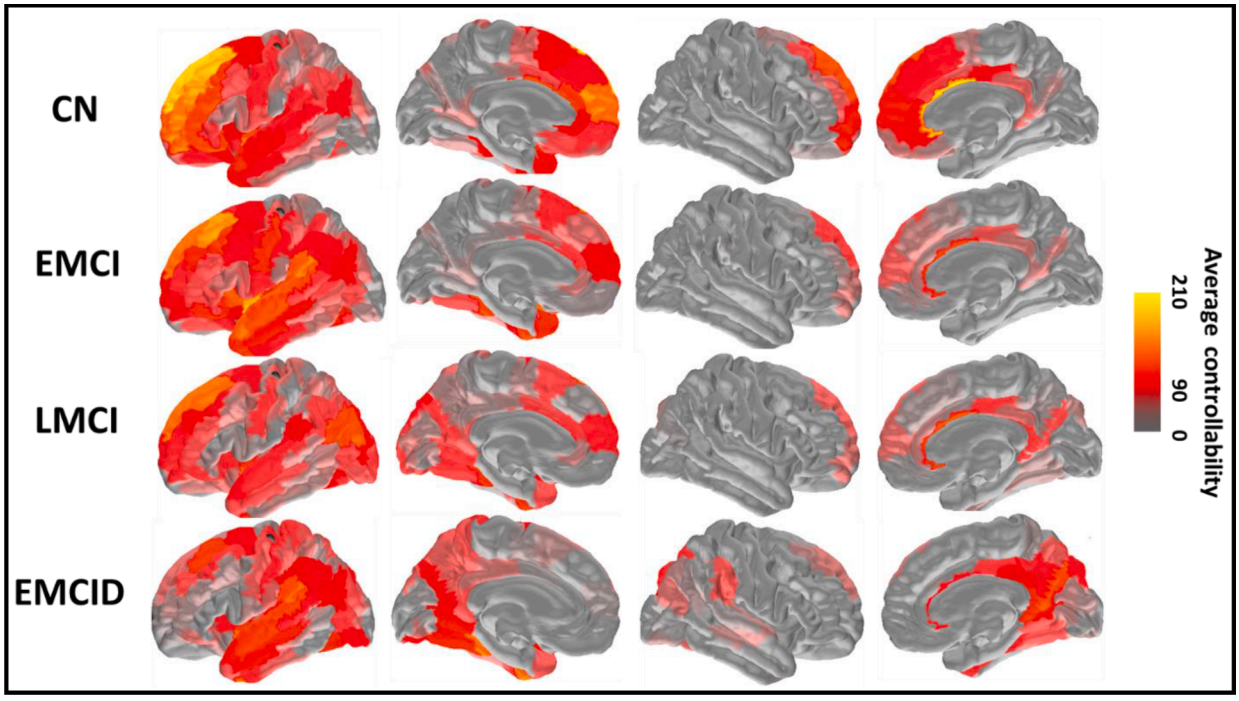

Fig. 2. Controllability distribution maps of different groups. The average controllability values, averaged across 15 participants in each group, and ranked for all 210 brain regions were plotted on a surface visualization.

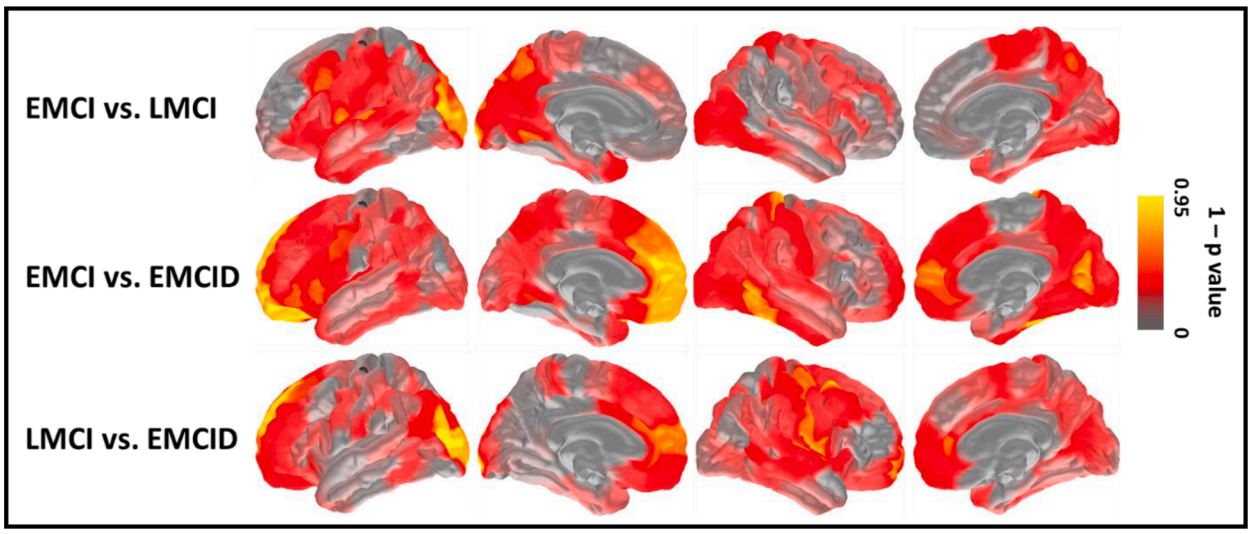

Fig. 3. Statistical comparison of controllability distribution between different MCI groups. The color bar indicates that only regions with yellow color on the top of the brain represent significant difference ($P < 0.05$) between different groups.

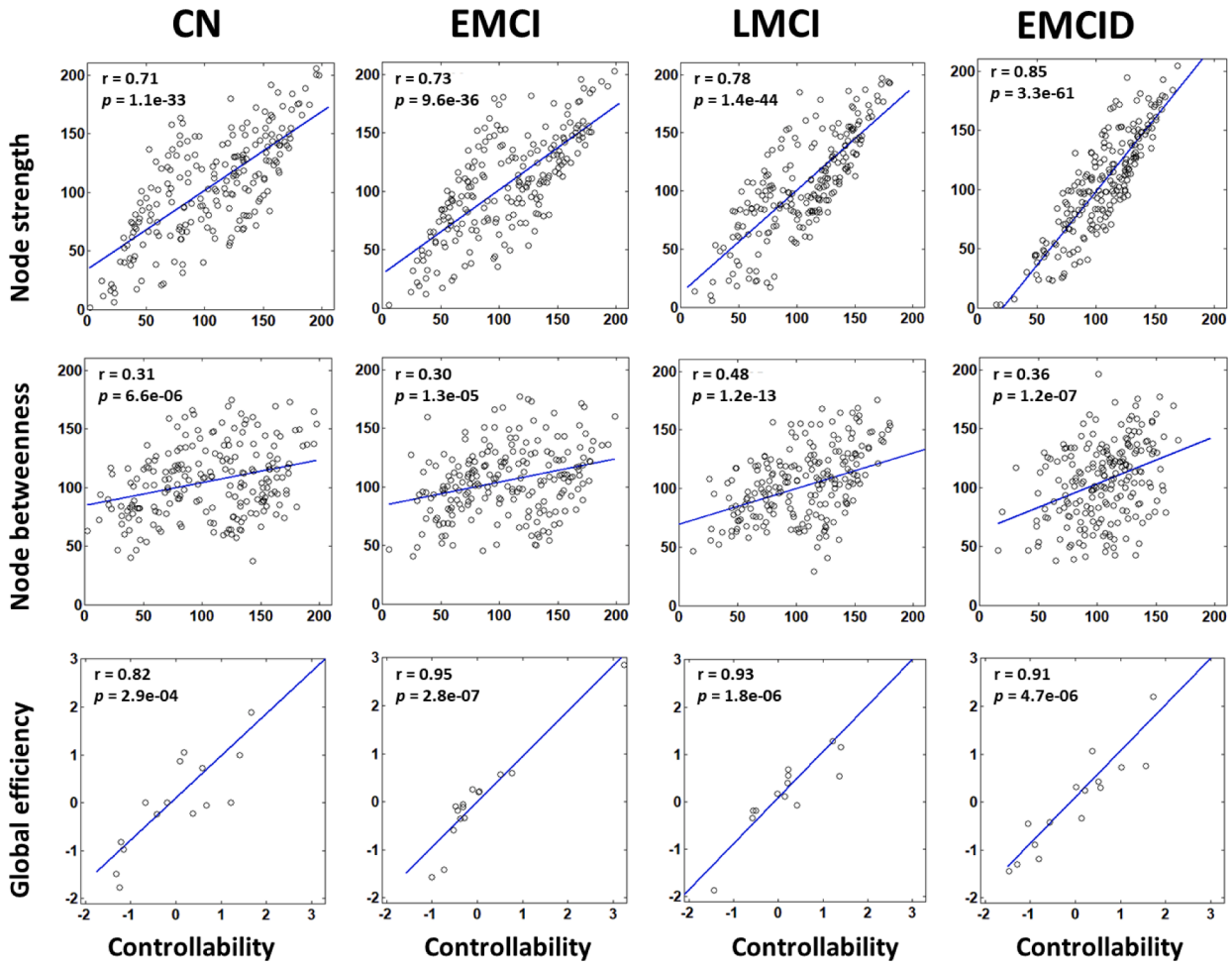

Fig. 4. Controllability versus graph measures. The first row represents the scatter plot of weighted node strength, averaged over participants in each group, respectively, versus average controllability. The second row represents the scatter plot of weighted node betweenness, averaged over participants in each group, respectively, versus average controllability. The third row represents the scatter plot of global efficiency versus controllability. The global efficiency was averaged over all brain regions of each participant, and then averaged over participants in each group, respectively.

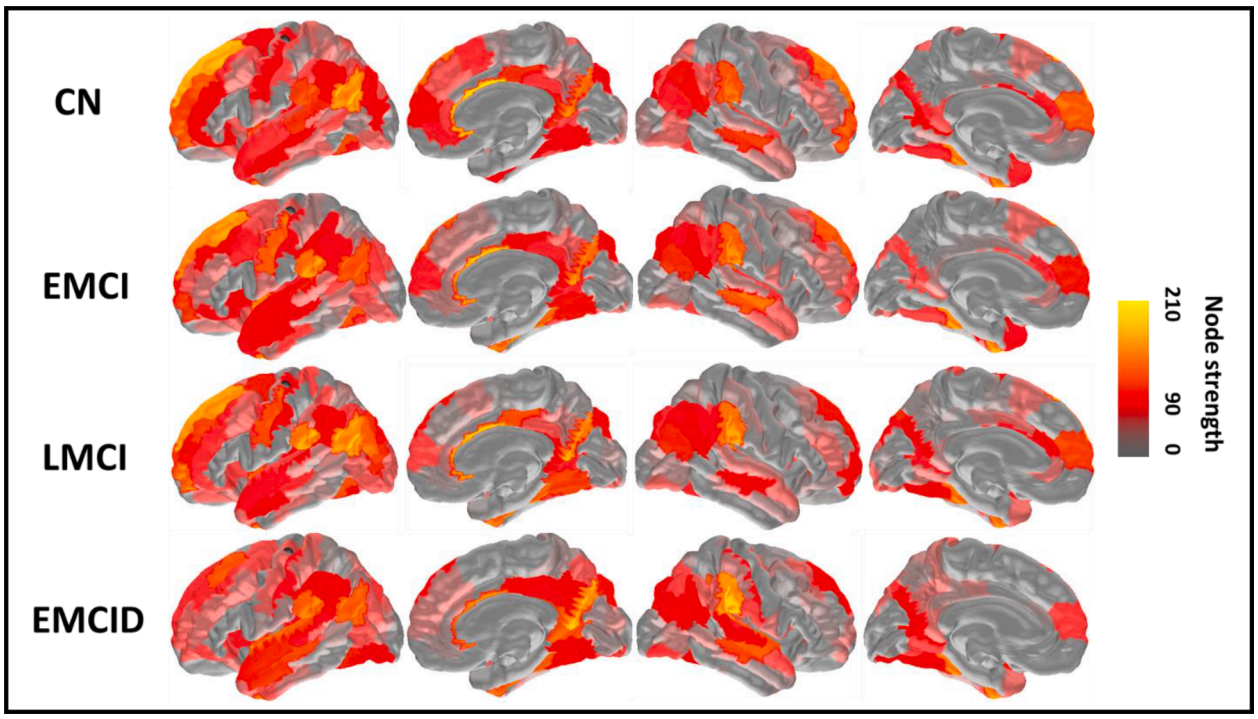

Fig. 5. Node strength distribution of different groups. The node strength values, averaged across 15 participants in each group, and ranked for all 210 brain regions were plotted on a surface visualization.

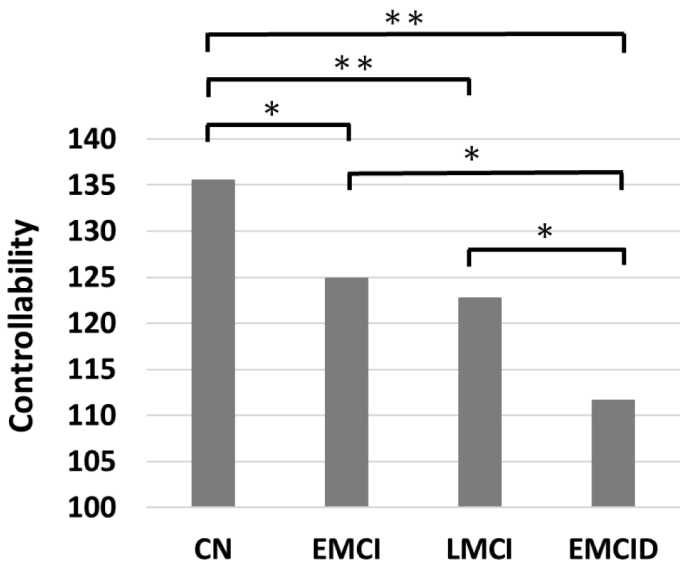

Fig. 6. Statistical comparison of controllability values in default mode network between different groups. "*" indicates $P < 0.05$ after FDR correction. "**" indicates $P < 0.01$ after FDR correction.

4. Discussion

The primary goal of this study is to investigate the neural alterations underlying brain network dynamics associated with mild depression in MCI patients from a systematic level via a novel brain controllability analysis. The average controllability matrix was applied to explore the control mechanisms underlying depressive symptoms in MCI patients. Average controllability was calculated from white matter connectivity in the context of the brain network control theory (Gu et al., 2015). The main findings in this study are that the brain average controllability of the default mode network of EMCID patients was significantly decreased compared to cognitively normal subjects, EMCI patients without depression, and even LMCI patients without depression. On the other hand, our results suggest that multiple brain regions, including the superior prefrontal, temporal, and cingulate cortices, are significantly altered in association with depressive symptom in EMCI patients. To the best of our knowledge, the present study represents the first effort to investigate the neural alterations underlying brain network transitions associated with depressive symptoms in MCI patients, and does so using novel brain controllability analyses.

Depression is one of the most common neuropsychiatric complications of EMCI, which can be seen as a set of related problems in cognitive-control (Pellegrino et al., 2013). Several studies, based on various neuroimaging modalities such as PET, fMRI, functional near-infrared spectroscopy (fNIRS), and electroencephalography (EEG), have employed traditional graph-based analysis to reveal abnormal properties of brain networks in depression and dementia patients (Lee et al., 2010,; Liu et al., 2017,; Byers and Yaffe, 2011,; Li et al., 2019,; Li et al., 2019,; Sun et al., 2019). Although most studies report local properties changed in both depression and dementia patients (Yu et al., 2019,; Lee et al., 2010,; Burke et al., 2019), it remains unclear how these regional changes lead to systematic-level alterations of the brain and depressive symptoms in dementia patients. Interestingly, our finding indicated that two graph measures of node strength and global efficiency were positively correlated with brain controllability measurement across all groups. This high correlation between node strength and controllability may imply the functional role of these regional hubs (high node strength) as critical for guiding the brain's movement from an arbitrary state to a desired state by appropriate choice of external or internal stimulus. Structurally, it also indicates that the brain regions with high average controllability towards the brain network system are mainly located in strongly connected areas. The highest correlation between node strength and controllability was in the EMCID group, which may further indicate a compensatory mechanism triggered in the cognitive-deficit brain networks. It is possible that an EMCID patient reduces the utilization of poorly functioning brain areas and focuses on the well-functioning regions to control the proceeding of brain

behaviors to compensate for the lost function of other brain regions. The strong correlation between global efficiency and controllability may imply that a brain with higher capacity for parallel information transfer among nodes contributes to a more controllable brain system by external stimuli. It also suggests that an easily controllable brain system requires the network to be more efficient in signal delivery. The brain's global efficiency has been related to the executive function during task performance (Reijmer et al., 2013). From the control perspective, our results imply that performing a task is highly related to the extent to which the brain can be modulated towards an intrinsic or external stimulus. The fact that the lowest correlation between global efficiency and controllability is in the cognitively normal subjects further supports a decrease of brain complexity in MCI patients (Sandu et al., 2014,; Wang et al., 2017). Therefore, even though a brain network may be structurally efficient, the overall brain may still be less controllable in MCI patients due to the brain's high complexity in cognitive normal subjects.

Depression and dementia-related studies suggest that the changes in the DMN are essential for explaining the disabling, and therefore intrinsically "depressive" and "dementing" natures, of the two diseases (Royall et al., 2013). Recently, the connectivity indices of DMN have been shown to be highest in normal controls, intermediate in MCI, and lowest in AD (Petrella et al., 2011). The same trend of decreased DMN connectivity has also been observed in depressed patients (Bluhm et al., 2009). Interestingly, from the control perspective, our findings indicate that the average controllability of DMN is also highest in cognitively normal subjects, intermediate in the EMCI and LMCI groups, and largely decreased in the EMCID group, indicating a loss of controlling capacity of DMN with the severity of the disease. The decreased controllability in DMN from cognitively normal subjects to E\LMCI groups is consistent with previous findings that deficits occurred in DMN throughout the progression of dementia (Lee et al., 2016). As the depressive symptoms develop in MCI patients, the ability of the DMN to transition the brain between different activated behaviors is further decreased, indicating a superposition of the effects from the two diseases. In the clinic, the EMCID patients usually have lower clinical scores than the EMCI patients so they are more likely to be categorized into an even worse cognitive group, like the LMCI group. Interestingly, our finding shows that the EMCID patients with depression have significantly reduced DMN controllability than the LMCI group, indicating the DMN changes due to MCI are smaller compared to those associated with depression. The overlay effects of the two diseases are also reported in other network-level studies, which demonstrate the decrease of global efficiency in MCI patients with depression when compared to the cognitively normal, MCI patients, and depression groups (Li et al., 2015). It is no surprise, then, that there is a decreased trend in controllability observed due to the high positive correlation between controllability and global efficiency as shown in Fig. 4. The DMN plays a critical role in controlling the preceding of the brain and trainsiting the brain into many task-based activation profiles, and relaxing back once the task has been done (Lin et al., 2017). Substantially decreased controllability of DMN in the EMCID group, may account for the loss of capability of depressive patients to initiate, maintain, and control their thoughts, behaviors, or emotions to change their brain states and produce desired outcomes, or avoiding an undesired outcome. Although the main focus of this study was to differentiate MCI patients with and without depression, our results also indicate the feasibility of using controllability diagnostic for early detection of MCI patients, which is also clinically important. The decreased connectivity of the DMN in MCI patients has been implicated in the loss of ability to maintain human memory in dementia (Lee et al., 2016,; Qi et al., 2010). From the control perspective, our results indicate that the controllability of DMN also shows a decreased trend from healthy subjects to the MCI patients, implying that the memory deficit in MCI patients was related to the disability of DMN in controlling the proceeding of the brain between different states or maintaining in a specific brain state.

Recently, alterations of structure and function in depressed patients have been shown in the frontal-temporal-parietal regions, particularly in the frontal areas (Bos et al., 2018). Such a changing pattern was also observed in MCI pathologic studies, which may further impede the differentiation between depression and MCI symptoms based on the traditional graph-based analysis (Sabbagh et al., 2010). From the systematic level, the present work revealed some crucial regions in differentiating the MCI patients with depressive symptoms from those who not (Fig. 7). For instance, the average controllability of the left superior prefrontal cortex differentiates between the CN group and EMCI group, between the EMCI group and EMCID group, and between the LMCI group and EMCID group. We observed a significant decreased trend of controllability from cognitively normal, to E/LMCI, then to the EMCID group. The prefrontal cortex dysfunction has been a central theme in the psychiatric neuroimaging literature (Masdeu, 2011). This region is involved in executive function, cognitive control, and planning (Koechlin and Summerfield, 2007,; Koechlin et al., 2003). The further attenuated controllability in the left superior prefrontal cortex of EMCID patients, relative to the E/LMCI patients, may explain the loss of ability for depressed patients to respond to cognitive control tasks, such as controlling emotion or setting and planning goals. The same localized impairment in network controllability of the left superior frontal cortex in subjects at high risk of bipolar suffering recurrent major depressive episodes was seen in previous study. (Jeganathan et al., 2018). The finding further suggests that the left prefrontal cortex's regional controllability may be a valuable biomarker for distinguishing depressive symptoms from MCI patients. The right superior prefrontal cortex in EMCID was also significantly decreased compared to cognitively normal subjects, which may explain the inability of depressed patients to establish and control the negative feelings. The same significantly decreased trend was not observed between cognitive normal and EMCI groups. This may also be used as a marker to differentiate the EMCI group from EMCID group, with one group showing a significant difference from the cognitively normal subjects. The l/r cingulate cortex in EMCID patients also displayed significantly decreased controllability versus the cognitively normal group. The cingulate cortex has been linked to cognitive control, negative affect and pain (Shackman et al., 2011). The deficit of controlling ability in the cingulate cortex of depressed patients may further enhance the disability of depression patients to control negative mood states. However, same significantly decreased controllability in right cingulate cortex was observed in the EMCI group, which may impede the differentiation between the EMCI and EMCID groups using the right cingulate cortex as biomarker. In conclusion, the regional controllability of left/right superior prefrontal cortex and the left cingulate cortex may be promising regional biomarkers to differentiate between EMCI and EMCID patients. The current work provides some promising biomarkers to distinguish between the CN, EMCI, EMCID, and LMCI groups. It is worth noting, however, that the inclusion of the LMCI group in the current study was done to ascertain whether the deficit shown in the early stage MCI group (EMCID) was caused by depression instead of the progression of dementia. However, it would be very interesting to include a group of LMCI patients with depression to compare the associations of depression across the stages of MCI patients, and this will be our plan for a future study.

5. Conclusion

In conclusion, our findings suggest that the brain controllability can be a potential biomarker to differentiate EMCI patients with depressive symptoms from those who are not depressed. The results also illustrate a significant decrease in controllability in the default mode network of EMCI patients with depression versus those EMCI patients without depression. The regional comparison also demonstrated that the regional controllability of the left/right superior prefrontal cortex and left cingulate cortex can be employed as promising biomarkers to differentiate the EMCI and EMCID patients.

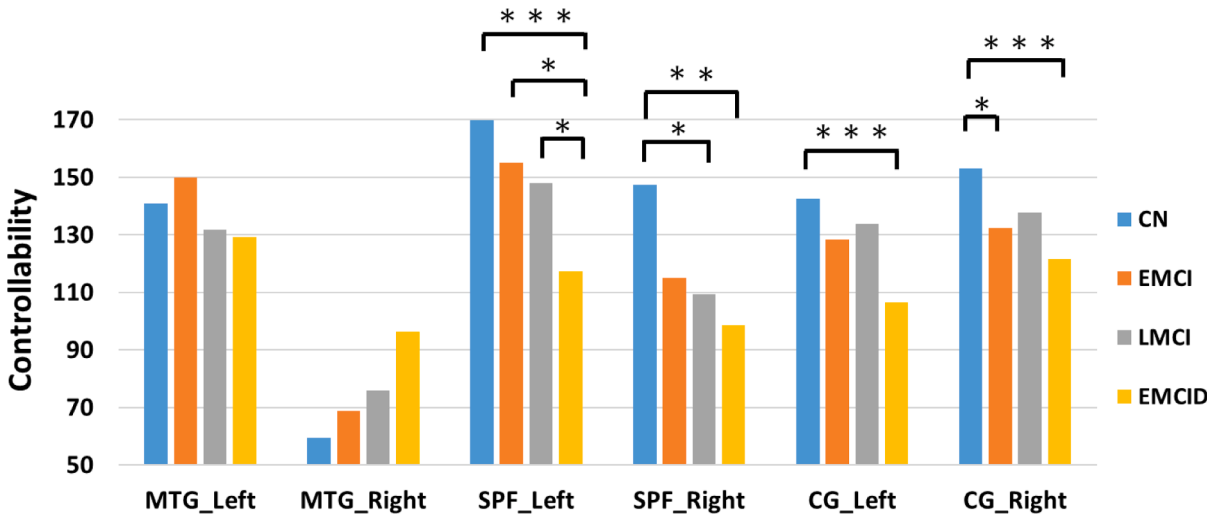

Fig. 7. Statistical comparison of regional controllability between different groups. The regions include left/right medial temporal gyrus (MTG), left/right superior prefrontal cortex (SPF), and left/right cingulate cortex (CG). "∗" indicates $P < 0.05$ after FDR correction. "∗∗" indicates $P < 0.01$ after FDR correction. . "∗∗∗" indicates $P < 0.005$ after FDR correction.

Author Contributions

FF analyzed and interpreted the data, summarized the results and was a major contributor in writing the manuscript. YG co-designed the study, assisted in analyzing data and interpreting the results, and also contributed to manuscript writing. PS assisted in interpretation of the results and manuscript revision. SS assisted in interpretation of the results and manuscript revision. YZ designed the study, assisted in analyzing data and interpreting the results, revised and finalized the manuscript. All authors read and approved the final manuscript.

CRediT authorship contribution statement

Feng Fang: Data curation, Formal analysis, Investigation, Methodology, Visualization, Writing – original draft. **Yunyuan Gao:** Conceptualization, Data curation, Formal analysis, Investigation, Methodology, Writing – review & editing. **Paul E. Schulz:** Investigation, Supervision, Validation, Writing – review & editing. **Sudhakar Selvaraj:** Supervision, Validation, Writing – review & editing. **Yingchun Zhang:** Conceptualization, Data curation, Formal analysis, Investigation, Methodology, Project administration, Resources, Software, Supervision, Validation, Writing – review & editing.

Declaration of Competing Interest

None.

Acknowledgements

The research is supported in part by the University of Houston. Data collection and sharing for this project was funded by the Alzheimer's Disease Neuroimaging Initiative (ADNI) (National Institutes of Health Grant U01 AG024904) and DOD ADNI (Department of Defense award number W81XWH-12-2-0012). ADNI is funded by the National Institute on Aging, the National Institute of Biomedical Imaging and Bioengineering, and through generous contributions from the following: AbbVie, Alzheimer's Association; Alzheimer's Drug Discovery Foundation; Araclon Biotech; BioClinica, Inc.; Biogen; Bristol-Myers Squibb Company; CereSpir, Inc.; Cogstate; Eisai Inc.; Elan Pharmaceuticals, Inc.; Eli Lilly and Company; EuroImmun; F. Hoffmann-La Roche Ltd and its affiliated company Genentech, Inc.; Fujirebio; GE Healthcare; IXICO Ltd.; Janssen Alzheimer Immunotherapy Research & Development, LLC.; Johnson & Johnson Pharmaceutical Research & Development LLC.; Lumosity; Lundbeck; Merck & Co., Inc.; Meso Scale Diagnostics, LLC.; NeuroRx Research; Neurotrack Technologies; Novartis Pharmaceuticals Corporation; Pfizer Inc.; Piramal Imaging; Servier; Takeda Pharmaceutical Company; and Transition Therapeutics. The Canadian Institutes of Health Research is providing funds to support ADNI clinical sites in Canada. Private sector contributions are facilitated by the Foundation for the National Institutes of Health (www.fnih.org). The grantee organization is the Northern California Institute for Research and Education, and the study is coordinated by the Alzheimer's Therapeutic Research Institute at the University of Southern California. ADNI data are disseminated by the Laboratory for Neuro Imaging at the University of Southern California.

References

A. s. Association, 2018. 2018 Alzheimer's disease facts and figures. Alzheimer's & Dement. 14, 367–429.
Minati, L., Edginton, T., Bruzzone, M.G., Giaccone, G., 2009. Reviews: current concepts in Alzheimer's disease: a multidisciplinary review. Am. J. Alzheimer's Dis. Other Dement.® 24, 95–121.
Li, R., Rui, G., Chen, W., Li, S., Schulz, P.E., Zhang, Y., 2018. Early detection of Alzheimer's disease using non-invasive near-infrared spectroscopy. Front. Aging Neurosci. 10, 366.
Luo, Y., Yang, W., Li, N., Yang, X., Zhu, B., Wang, C., et al., 2020. Anodal transcranial direct current stimulation can improve spatial learning and memory and attenuate Aβ42 burden at the early stage of Alzheimer's Disease in APP/PS1 transgenic mice. Front. Aging Neurosci. 12.
Luo, Y., Sun, Y., Tian, X., Zheng, X., Wang, X., Li, W., et al., 2021. Deep brain stimulation for Alzheimer's disease: stimulation parameters and potential mechanisms of action. Front. Aging Neurosci. 13, 104.
Chi, S., Yu, J.-T., Tan, M.-S., Tan, L., 2014. Depression in Alzheimer's disease: epidemiology, mechanisms, and management. J. Alzheimers Dis. 42, 739–755.
A. P. Association, 2013. Diagnostic and Statistical Manual of Mental Disorders (DSM-5®). American Psychiatric Pub.
Dillon, C., Tartaglini, M.F., Stefani, D., Salgado, P., Taragano, F.E., Allegri, R.F., 2014. Geriatric depression and its relation with cognitive impairment and dementia. Arch. Gerontol. Geriatr. 59, 450–456.
Ownby, R.L., Crocco, E., Acevedo, A., John, V., Loewenstein, D., 2006. Depression and risk for Alzheimer disease: systematic review, meta-analysis, and metaregression analysis. Arch. Gen. Psychiatry 63, 530–538.
Beason-Held, L.L., Goh, J.O., An, Y., Kraut, M.A., O'Brien, R.J., Ferrucci, L., et al., 2013. Changes in brain function occur years before the onset of cognitive impairment. J. Neurosci. 33, 18008–18014.
Yu, Y., Li, Z., Lin, Y., Yu, J., Peng, G., Zhang, K., et al., 2019. Depression affects intrinsic brain activity in patients with mild cognitive impairment. Front. Neurosci. 13, 1333.
Lee, H.S., Choo, I.H., Lee, D.Y., Kim, J.W., Seo, E.H., Kim, S.G., et al., 2010. Frontal dysfunction underlies depression in mild cognitive impairment: a FDG-PET study. Psychiatry Investig. 7, 208.
Liu, J., Li, M., Pan, Y., Lan, W., Zheng, R., Wu, F.-X., et al., 2017. Complex brain network analysis and its applications to brain disorders: a survey. Complexity 2017.

Byers, A.L., Yaffe, K., 2011. Depression and risk of developing dementia. Nat. Rev. Neurol. 7, 323.
Fang, F., Potter, T., Nguyen, T., Zhang, Y., 2020. Dynamic reorganization of the cortical functional brain network in affective processing and cognitive reappraisal. Int. J. Neural Syst. 30, 2050051. -2050051.
Nguyen, T., Zhou, T., Potter, T., Zou, L., Zhang, Y., 2019. The cortical network of emotion regulation: insights from advanced EEG-fMRI integration analysis. IEEE Trans. Med. Imaging 38, 2423–2433.
Sporns, O., 2018. Graph theory methods: applications in brain networks. Dialogues Clin. Neurosci. 20, 111.
Tumati, S., Marsman, J.-B.C., De Deyn, P.P., Martens, S., Aleman, A., 2020. Functional network topology associated with apathy in Alzheimer's disease. J. Affect. Disord. 266, 473–481.
Lin, P., Yang, Y., Gao, J., De Pisapia, N., Ge, S., Wang, X., et al., 2017. Dynamic default mode network across different brain states. Sci. Rep. 7, 1–13.
Gu, S., Pasqualetti, F., Cieslak, M., Telesford, Q.K., Alfred, B.Y., Kahn, A.E., et al., 2015. Controllability of structural brain networks. Nat. Commun. 6, 1–10.
Öngür, D., Lundy, M., Greenhouse, I., Shinn, A.K., Menon, V., Cohen, B.M., et al., 2010. Default mode network abnormalities in bipolar disorder and schizophrenia. Psychiatry Res. 183, 59–68.
Greicius, M.D., Supekar, K., Menon, V., Dougherty, R.F., 2009. Resting-state functional connectivity reflects structural connectivity in the default mode network. Cereb. Cortex 19, 72–78.
Guo, Z., Liu, X., Hou, H., Wei, F., Liu, J., Chen, X., 2016. Abnormal degree centrality in Alzheimer's disease patients with depression: A resting-state functional magnetic resonance imaging study. Exp. Gerontol. 79, 61–66.
Fang, P., Zeng, L.-L., Shen, H., Wang, L., Li, B., Liu, L., et al., 2012. Increased cortical-limbic anatomical network connectivity in major depression revealed by diffusion tensor imaging. PLoS One 7, e45972.
Korgaonkar, M.S., Cooper, N.J., Williams, L.M., Grieve, S.M., 2012. Mapping inter-regional connectivity of the entire cortex to characterize major depressive disorder: a whole-brain diffusion tensor imaging tractography study. Neuroreport 23, 566–571.
Burke, A.D., Goldfarb, D., Bollam, P., Khokher, S., 2019. Diagnosing and treating depression in patients with Alzheimer's disease. Neurol. Therapy 1–26.
Bai, F., Shu, N., Yuan, Y., Shi, Y., Yu, H., Wu, D., et al., 2012. Topologically convergent and divergent structural connectivity patterns between patients with remitted geriatric depression and amnestic mild cognitive impairment. J. Neurosci. 32, 4307–4318.
Wise, T., Marwood, L., Perkins, A., Herane-Vives, A., Joules, R., Lythgoe, D., et al., 2017. Instability of default mode network connectivity in major depression: a two-sample confirmation study. Transl. Psychiatry 7, e1105. -e1105.
Royall, D.R., Palmer, R.F., Vidoni, E.D., Honea, R.A., 2013. The default mode network may be the key substrate of depressive symptom-related cognitive changes. J. Alzheimers Dis. 34, 547–560.
Tang, E., Giusti, C., Baum, G.L., Gu, S., Pollock, E., Kahn, A.E., et al., 2017. Developmental increases in white matter network controllability support a growing diversity of brain dynamics. Nat. Commun. 8, 1–16.
Menara, T., Bassett, D.S., Pasqualetti, F., 2018. Structural controllability of symmetric networks. IEEE Trans. Autom. Control 64, 3740–3747.
Strauman, T.J., Eddington, K.M., 2017. Treatment of depression from a self-regulation perspective: basic concepts and applied strategies in self-system therapy. Cogn. Ther. Res. 41, 1–15.
Taquet, M., Quoidbach, J., Gross, J.J., Saunders, K.E., Goodwin, G.M., 2020. Mood homeostasis, low mood, and history of depression in 2 large population samples. JAMA Psychiatry 77, 944–951.
Li, B.J., Friston, K., Mody, M., Wang, H.N., Lu, H.B., Hu, D.W., 2018. A brain network model for depression: from symptom understanding to disease intervention. CNS Neurosci. Ther. 24, 1004–1019.
Scale, G.D., 1997. Geriatric Depression Scale. Arch. Intern. Med. 157, 449–454.
McGuire, B.E., Batchelor, J., 1998. Inter-rater reliability of the WMS-R logical memory and visual reproduction subtests in a neurosurgical sample. Aust. Psychol. 33, 231–233.
Edmonds, E.C., McDonald, C.R., Marshall, A., Thomas, K.R., Eppig, J., Weigand, A.J., et al., 2019. Early versus late MCI: Improved MCI staging using a neuropsychological approach. Alzheimer's Dement. 15, 699–708.
Yeh, F.-C., Tseng, W.-Y.I., 2011. NTU-90: a high angular resolution brain atlas constructed by q-space diffeomorphic reconstruction. Neuroimage 58, 91–99.
Sakha, M.S., Shaker, H.R., 2017. Optimal sensors and actuators placement for large-scale unstable systems via restricted genetic algorithm. Eng. Comput.
Sreeram, V., Agathoklis, P., 1994. On the properties of Gram matrix. IEEE Trans. Circuits Syst. I 41, 234–237.
Berlot, R., Metzler-Baddeley, C., Ikram, M.A., Jones, D.K., O'Sullivan, M.J., 2016. Global efficiency of structural networks mediates cognitive control in mild cognitive impairment. Front. Aging Neurosci. 8, 292.
Rubinov, M., Sporns, O., 2010. Complex network measures of brain connectivity: uses and interpretations. Neuroimage 52, 1059–1069.
Woolson, R., 2007. Wilcoxon signed-rank test. Wiley Encycl. Clin. Trials 1–3.
Poole, M.A., O'Farrell, P.N., 1971. The assumptions of the linear regression model. Trans. Inst. Br. Geogr. 145–158.
Benjamini, Y., Hochberg, Y., 1995. Controlling the false discovery rate: a practical and powerful approach to multiple testing. J. R. Statist. Soc. 57, 289–300.
Pellegrino, L.D., Peters, M.E., Lyketsos, C.G., Marano, C.M., 2013. Depression in cognitive impairment. Curr. Psychiatry Rep. 15, 384.
Li, R., Rui, G., Zhao, C., Wang, C., Fang, F., Zhang, Y., 2019. Functional network alterations in patients with amnestic mild cognitive impairment characterized using functional near-infrared spectroscopy. IEEE Trans. Neural Syst. Rehabil. Eng. 28, 123–132.
Li, R., Nguyen, T., Potter, T., Zhang, Y., 2019. Dynamic cortical connectivity alterations associated with Alzheimer's disease: an EEG and fNIRS integration study. NeuroImage 21, 101622.
Sun, S., Li, X., Zhu, J., Wang, Y., La, R., Zhang, X., et al., 2019. Graph theory analysis of functional connectivity in major depression disorder with high-density resting state EEG data. IEEE Trans. Neural Syst. Rehabil. Eng. 27, 429–439.
Reijmer, Y.D., Leemans, A., Caeyenberghs, K., Heringa, S.M., Koek, H.L., Biessels, G.J., et al., 2013. Disruption of cerebral networks and cognitive impairment in Alzheimer disease. Neurology 80, 1370–1377.
Sandu, A.-L., Staff, R.T., McNeil, C.J., Mustafa, N., Ahearn, T., Whalley, L.J., et al., 2014. Structural brain complexity and cognitive decline in late life—a longitudinal study in the Aberdeen 1936 Birth Cohort. Neuroimage 100, 558–563.
Wang, B., Niu, Y., Miao, L., Cao, R., Yan, P., Guo, H., et al., 2017. Decreased complexity in Alzheimer's disease: resting-state fMRI evidence of brain entropy mapping. Front. Aging Neurosci. 9, 378.
Petrella, J., Sheldon, F., Prince, S., Calhoun, V.D., Doraiswamy, P., 2011. Default mode network connectivity in stable vs progressive mild cognitive impairment. Neurology 76, 511–517.
Bluhm, R., Williamson, P., Lanius, R., Théberge, J., Densmore, M., Bartha, R., et al., 2009. Resting state default-mode network connectivity in early depression using a seed region-of-interest analysis: decreased connectivity with caudate nucleus. Psychiatry Clin. Neurosci. 63, 754–761.
Lee, E.-S., Yoo, K., Lee, Y.-B., Chung, J., Lim, J.-E., Yoon, B., et al., 2016. Default mode network functional connectivity in early and late mild cognitive impairment. Alzheimer Dis. Assoc. Disord. 30, 289–296.
Li, W., Ward, B.D., Liu, X., Chen, G., Jones, J.L., Antuono, P.G., et al., 2015. Disrupted small world topology and modular organisation of functional networks in late-life depression with and without amnestic mild cognitive impairment. J. Neurol., Neurosurg. Psychiatry 86, 1097–1105.
Qi, Z., Wu, X., Wang, Z., Zhang, N., Dong, H., Yao, L., et al., 2010. Impairment and compensation coexist in amnestic MCI default mode network. Neuroimage 50, 48–55.
Bos, M.G., Peters, S., van de Kamp, F.C., Crone, E.A., Tamnes, C.K., 2018. Emerging depression in adolescence coincides with accelerated frontal cortical thinning. J. Child Psychol. Psychiatry 59, 994–1002.
Sabbagh, M.N., Cooper, K., DeLange, J., Stoehr, J.D., Thind, K., Lahti, T., et al., 2010. Functional, global and cognitive decline correlates to accumulation of Alzheimer's pathology in MCI and AD. Curr. Alzheimer Res. 7, 280–286.
Masdeu, J.C., 2011. Neuroimaging in psychiatric disorders. Neurotherapeutics 8, 93–102.
Koechlin, E., Summerfield, C., 2007. An information theoretical approach to prefrontal executive function. Trends Cogn. Sci. 11, 229–235.
Koechlin, E., Ody, C., Kouneiher, F., 2003. The architecture of cognitive control in the human prefrontal cortex. Science 302, 1181–1185.
Jeganathan, J., Perry, A., Bassett, D.S., Roberts, G., Mitchell, P.B., Breakspear, M., 2018. Fronto-limbic dysconnectivity leads to impaired brain network controllability in young people with bipolar disorder and those at high genetic risk. NeuroImage 19, 71–81.
Shackman, A.J., Salomons, T.V., Slagter, H.A., Fox, A.S., Winter, J.J., Davidson, R.J., 2011. The integration of negative affect, pain and cognitive control in the cingulate cortex. Nat. Rev. Neurosci. 12, 154–167.